BJR

Received: 17 June 2014 | Revised: 17 August 2015 | Accepted: 1 October 2015

doi: 10.1259/bjr.20140434

Cite this article as:
Wu J, Zhu Q, Zhu W, Chen W, Wang S. Comparative study of CT appearances in mucinous tubular and spindle cell carcinoma and collecting duct carcinoma of the kidney. *Br J Radiol* 2015; **88**: 20140434.

FULL PAPER

Comparative study of CT appearances in mucinous tubular and spindle cell carcinoma and collecting duct carcinoma of the kidney

JINGTAO WU, PhD, MD, QINGQIANG ZHU, PhD, WENRONG ZHU, PhD, WENXIN CHEN, PhD and SHOUAN WANG, MD

Department of Medical Imaging, Subei People's Hospital, Medical School of Yangzhou University, Yangzhou, China

Address correspondence to: Prof. Jingtao Wu
E-mail: *wujingtaodoctor@163.com*

Jingtao Wu and Qingqiang Zhu contributed equally to this work.

Objective: To characterize the multidetector CT (MDCT) imaging characteristics of mucinous tubular and spindle cell carcinoma (MTSCC) and collecting duct carcinoma (CDC) of the kidney.
Methods: 21 patients with MTSCC and 18 patients with CDC were studied retrospectively. MDCT was undertaken to investigate differences in tumour characteristics.
Results: Five patients with MTSCC had calcifications as did nine patients with CDC ($p = 0.108$). In three patients with MTSCC and four patients with CDC, the tumours had a clear boundary ($p = 0.682$). No patient with MTSCC had retroperitoneal lymph node metastasis as did five patients with CDC ($p = 0.015$). 16 patients with MTSCC showed homogeneous enhancement, whereas 11 patients with CDC showed heterogeneous enhancement ($p = 0.025$). The attenuation value of CDC tumours was greater than that of MTSCC and normal renal parenchyma on an unenhanced CT ($p = 0.027$). MTSCC and CDC tumour enhancement was less than the normal renal cortex and medulla in all phases ($p < 0.001$). Tumour enhancement was greater for CDC than that for MTSCC in all phases ($p = 0.011$, $p = 0.006$ and $p = 0.052$).
Conclusion: Unenhanced and dynamic MDCT may aid in diagnosis and differentiation of MTSCC and CDC of the kidney.
Advances in knowledge: This is the first series evaluating the imaging findings of MTSCC and CDC of which we are aware, and identification of such findings may improve diagnosis of these two rare tumours.

INTRODUCTION

Mucinous tubular and spindle cell carcinoma (MTSCC) and collecting duct carcinoma (CDC) are both uncommon subtypes of renal cell carcinoma (RCC).[1] MTSCC and CDC have been described to affect primarily adults. MTSCC is more common in females, whereas CDC is more common in males. Symptoms with both tumour types may include backache, abdominal pain and fever, although patients are commonly asymptomatic, and they are found incidentally.[1,2] CDCs develop from the distal segment of the collecting duct in the renal medullary pyramids and are indistinguishable from MTSCC on imaging studies. MTSCC and CDC share similar oncogenic and histological features and some imaging findings such as their medullary location, the attenuation of tumour, hypovascular enhancement pattern, infiltrative pattern of growth etc.[2] Despite these common features, MTSCC and CDC exhibit differences in prognosis. MTSCC is an RCC subtype with overall favourable prognosis compared with other RCCs, including slower growth and significantly lower rates of metastases, progression and death. Nephron-sparing surgery has been recommended for MTSCC by many authors,[2,3] with many studies increasingly confirming good long-term results and excellent patient survival.[3] By contrast, a radical operation is advocated by many surgeons for CDC.[3] The typical CDCs have a poor prognosis with many being metastatic at presentation. About two-thirds of patients die of their disease within 2 years of diagnosis.[4] Therefore, an accurate diagnosis is important for guiding the clinical treatment. The purpose of the present study was to retrospectively characterize multidetector CT (MDCT) characteristics, which lead to the histological diagnosis of MTSCC and CDC.

METHODS AND MATERIALS

Patients

This study was approved by the institutional research ethics committee. A retrospective search of pathology records and picture archiving and communications system identified 21 patients with MTSCC and 18 patients with CDC, who

were hospitalized at Subei People's Hospital between 2001 and 2014. Details of patients' age, gender, tumour size, surgery or biopsy confirmation, metastasis and clinical symptoms were recorded.

CT imaging technique

CT examinations were performed by using 16-slice [LightSpeed® Ultra; GE Healthcare, Milwaukee, WI ($n = 7$)] or 64-slice [Somatom® Definition; Siemens AG, Medical Solutions, Forchheim, Germany ($n = 32$)] detector row scanners. 19 cases with MTSCC and 17 cases with CDC underwent unenhanced precontrast CT scan, and all patients underwent contrast-enhanced CT scan. Parameters included detector collimation of 64.0×0.6 mm, gantry rotation time of 0.5 s, pitch of 1.4, tube voltage of 120 kVp and abdominal reference tube current of 230 mAs. All images were reconstructed from the contrast-enhanced CT scan with 0.75-mm slice thickness and 0.5-mm reconstruction increment. Contrast-enhanced CT scan was started by continuously injecting a bolus of 80–100 ml of iopromide (320 mg ml^{-1}; Schering, Berlin, Germany) followed by 40 ml of saline solution into an antecubital vein *via* an 18-gauge catheter (injection rate 5 ml s^{-1}). Unenhanced imaging was performed before administering the intravenous contrast agent. The enhanced CT scans began after 20 s for the arterial phase (cortical phase), 65 s for the corticomedullary phase (medullary phase) and 300 s for the excretory phase (delayed phase).

Pathological examination

At surgery and gross evaluation, specimens were assessed for shape; cystic components; fibrous capsule; invasion into the renal calyx, pelvis or ureter; and invasion into the renal vein or inferior vena cava. All renal tumours were confirmed to be MTSCC or CDC by pathology and immunohistology.

Imaging analysis and statistics

Two radiologists with more than 10 years' experience each, blinded to the final diagnosis, reviewed the CT images in consensus at a picture archiving and communication system workstation. The imaging parameters included tumour position, size, cystic or necrotic component, calcification, tumour attenuation on unenhanced CT scans, lymphadenopathy, perinephric stranding, hydronephrosis, presence or absence of a clear tumour boundary (capsule sign), vascular invasion and metastasis. The degree of enhancement [in Hounsfield units (HU)] on different phases of the enhanced CT scans was thereafter assessed.

Infiltrative growth was characterized by the lack of clear circumscriptions. However, expansive growth was defined as well-marginated, bulging tumour circumscriptions that displaced the normal renal parenchyma.

For the tumour, the measured area (the region of interest) was at the centre of the mass in order to avoid partial volume effects; however, intratumoral calcification and cystic components if present were avoided. Unenhanced tumour HU was classified as mildly high if >10 HU and high if >20 HU compared with normal renal parenchyma.

The normal renal cortex and medulla were measured in uninvolved unilateral renal cortex and medulla. 10-mm regions of interest were measured three times for each phase, and the mean value was used. The enhancement pattern of the tumour was classified as homogeneous or heterogeneous.

Statistical analysis

Statistical analysis used SPSS® v. 13.0 statistical software (IBM Corp., New York, NY; formerly SPSS Inc., Chicago, IL). Data are expressed as mean ± standard deviation, and count data are expressed as percentage. Evaluated characteristics were compared using χ^2 test, Fisher's exact test, independent-samples *t* test, analysis of variance and *post hoc* test (Tukey). Values of $p < 0.05$ were considered statistically significant.

RESULTS

Clinical and CT imaging features of mucinous tubular and spindle cell carcinoma and collecting duct carcinoma

The study included 21 patients (14 females and 7 males) with MTSCC and 18 patients (8 females and 10 males) with CDC. The mean age at diagnosis was slightly lower for patients with MTSCC (46.3 years; range, 29–67 years) than for those with CDC (48.8 years; range 20–67 years, $p = 0.732$). The presenting symptoms of MTSCC and CDC included flank pain (nine patients with MTSCC and eight patients with CDC), haematuria (six patients with CDC), palpable mass (three patients with CDC) and fever (seven patients with MTSCC and four patients with CDC).

19 patients (90%) with MTSCC and 18 patients (100%) with CDC had single tumours ($p = 0.490$). 20 patients with MTSCC and 16 patients with CDC had solid tumours (95% *vs* 89%, $p = 0.586$, Table 1). Cystic components were visible in 7 patients with MTSCC and 11 patients with CDC (33% *vs* 61%, $p = 0.113$, Table 1). There was evidence of calcifications in five patients with MTSCC tumours and nine patients with CDC tumours (24% *vs* 50%, $p = 0.108$, Table 1). In three patients with MTSCC and four patients with CDC, the tumours had a clear boundary (14% *vs* 22%, $p = 0.682$). 16 patients with MTSCC (76%) showed homogeneous enhancement, whereas 11 patients with CDC (61%) showed heterogeneous enhancement ($p = 0.025$). No patient with MTSCC had retroperitoneal lymph node metastasis as did five patients with CDC ($p = 0.015$). The tumour compressed the renal pelvis in 10 patients with MTSCC and 11 patients with CDC (48% *vs* 61%, $p = 0.523$). On unenhanced CT, the attenuation of MTSCC (32.3 ± 2.8 HU) was lower than that of CDC (46.7 ± 2.9 HU, $p = 0.013$), normal renal cortex (35.1 ± 4.2 HU, $p = 0.046$) and medulla attenuations (33.9 ± 3.1 HU, $p = 0.069$). MTSCC and CDC tumour enhancement was less than the enhancement of normal renal cortex and medulla, in all phases ($p < 0.001$, Table 2). Tumour enhancement was greater with CDC than that with MTSCC, in all phases ($p = 0.011$, $p = 0.006$ and $p = 0.052$, respectively, Table 2).

Surgical/gross observation and follow-up

21 patients (100%) with MTSCC underwent surgery. In 18 cases (86%), the masses were oval; 3 masses (14%) were irregular in

Table 1. Mass locations and CT findings in MTSCC and CDC

Main CT findings	MTSCC ($n = 21$)	CDC ($n = 18$)	p-value
Solitary mass	19	18	0.490
Solid mass	20	16	0.586
Cystic components	7	11	0.113
Calcifications	5	9	0.108
Capsule sign	3	4	0.682
Centred in the medulla	19	16	1.000
Compressed the renal pelvis	10	11	0.523
Haemorrhage	1	9	0.002
Homogeneous enhancement	16	7	0.025
Lymph node metastasis	0	5	0.015

CDC, collecting duct carcinoma; MTSCC, mucinous tubular and spindle cell carcinoma.
Data are given as the number of patients (n).

shape and 7 masses (33%) had small cystic components. Neither lymph node nor distant metastasis was found. In three cases (14%), the tumours were surrounded by fibrous capsules. They underwent total nephrectomy with a satisfactory outcome. No adjuvant therapy was given, and they were alive without manifesting disease or any other signs or symptoms during 5–13 years of follow-up.

18 patients (100%) with CDC underwent surgery. In 17 cases (94%), the masses were oval; 1 mass (5%) was irregular in shape and 11 masses (61%) had cystic components. Five patients with CDC (28%) had retroperitoneal lymph node metastasis. Nine patients (50%) had haemorrhage. In four cases (22%), the tumours were surrounded by fibrous capsules. In this study, all 18 patients with CDC underwent radical nephrectomy, and 17 patients (94%) could be followed up. Seven patients (39%) expired within 5 years of the initial diagnosis, while the others are still alive.

There was no evidence of invasion into the renal pelvis or calyx, renal vein, inferior vena cava or ureter with either disease.

Pathological findings

Microscopic sections of MTSCC tumour from two different patients are shown in Figures 1 and 2, respectively. Histological analysis indicated that MTSCC tumour cells showed tubular and spindle cell areas together with mucinous or myxoid stroma (Figures 1d and 2c). Immunochemistry staining demonstrated positive CK18 (+++, $n = 21$), vimentin (++, $n = 21$), cytokeratin 19 (CK19) (++, $n = 18$), 34βE12 (+++, $n = 17$) and CK AE1/AE3 (++, $n = 19$). Haemorrhage or desmoplasia were not found in any of our cases with MTSCC.

Microscopic sections of CDC tumour from two different patients are shown in Figures 3 and 4, respectively. Histological analysis indicated that CDC tumour cells showed tubular, papillary, tubulopapillary, pseudopapillary, cribriform and solid patterns (Figures 3d and 4d). Immunochemistry demonstrated positive vimentin (++, $n = 16$), CK8/18 (++, $n = 16$), 34βE12 (+++, $n = 12$) and CK19 (++, $n = 14$). Haemorrhage was found in nine cases with CDC (50%).

DISCUSSION

MTSCC is a rare low-grade polymorphic renal epithelial neoplasms with mucinous tubular and spindle cell features.[3] Histologically, they are composed of tightly packed, small, elongated tubules separated by pale mucinous stroma.[4] These tumours have a complex immunophenotype and stain for a wide variety of cytokeratins. Our pathological analysis showed clear positivity for CK proteins, such as CK18, in all cases we examined.

Table 2. CT attenuation of the renal cortex, medulla, MTSCC and CDC

Phase	Renal cortex ($n = 36$)	Renal medulla ($n = 36$)	MTSCC ($n = 21$)	CDC[a] ($n = 18$)	p-value
Unenhanced[b]	35.1 ± 4.2	33.9 ± 3.1	32.3 ± 2.8	46.7 ± 2.9	0.027
Corticomedullary	189.7 ± 8.3	77.9 ± 5.3	49.2 ± 4.7	66.1 ± 5.8	<0.001
Nephrographic	199.8 ± 11.6	117.3 ± 8.6	69.9 ± 8.1	93.8 ± 9.7	<0.001
Delayed	107.8 ± 7.9	97.3 ± 6.1	59.2 ± 6.1	63.2 ± 6.3	<0.001

CDC, collecting duct carcinoma; MTSCC, mucinous tubular and spindle cell carcinoma.
[a]Enhancement was higher in CDC than in MTSCC, in all phases ($p = 0.011$, $p = 0.006$ and $p = 0.052$, respectively).
[b]On unenhanced CT, attenuation of MTSCC was lower than that of CDC, the renal cortex and the medulla ($p = 0.013$, $p = 0.046$ and $p = 0.069$, respectively).

Figure 1. (a–d) Mucinous tubular and spindle cell carcinoma of the right kidney in a 59-year-old male. Axial unenhanced CT image (a) shows a poorly defined hypodense mass (arrow) in the medulla. The attenuation of the mass was 29 HU. Axial contrast-enhanced CT image acquired in the corticomedullary phase (b) shows mild enhancement (47 HU), which is less than the enhancement seen in the cortex and the medulla; tumour boundary is unclear (arrow). Axial image in (c) shows slightly increased attenuation of the tumour (61 HU, arrow) in the nephrographic phase. Haematoxylin and eosin staining of the tumour (d) shows tubular and spindle cell pattern (original magnification, ×400).

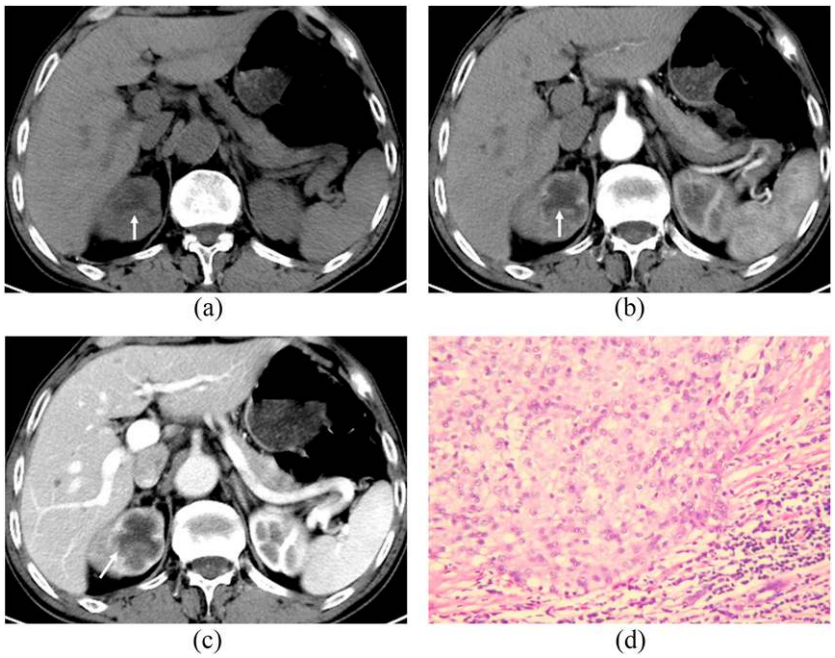

CDC constitutes <1% of all RCCs and is characterized by irregular angulated infiltration of the collecting duct tubules with desmoplastic stroma.[5] Approximately 100 cases with CDC have been reported previously in the literature; mean age at diagnosis is 55 years, although it varies over a wide range, and there is a 2:1 male predominance.[6] Histopathologically, CDC shows

Figure 2. (a–c) Mucinous tubular and spindle cell carcinoma of the left kidney in a 60-year-old male. Axial contrast-enhanced CT image acquired in the corticomedullary phase (a) shows mild enhancement (50 HU), which is less than the enhancement in the cortex and the medulla; tumour boundary is unclear (arrows). Axial image (b) shows slightly increased attenuation of the tumour (69 HU, arrows) in the nephrographic phase together with cystic components. Haematoxylin and eosin staining (c) shows the presence of tubular and spindle cell areas together with mucinous or myxoid stroma (original magnification, ×400).

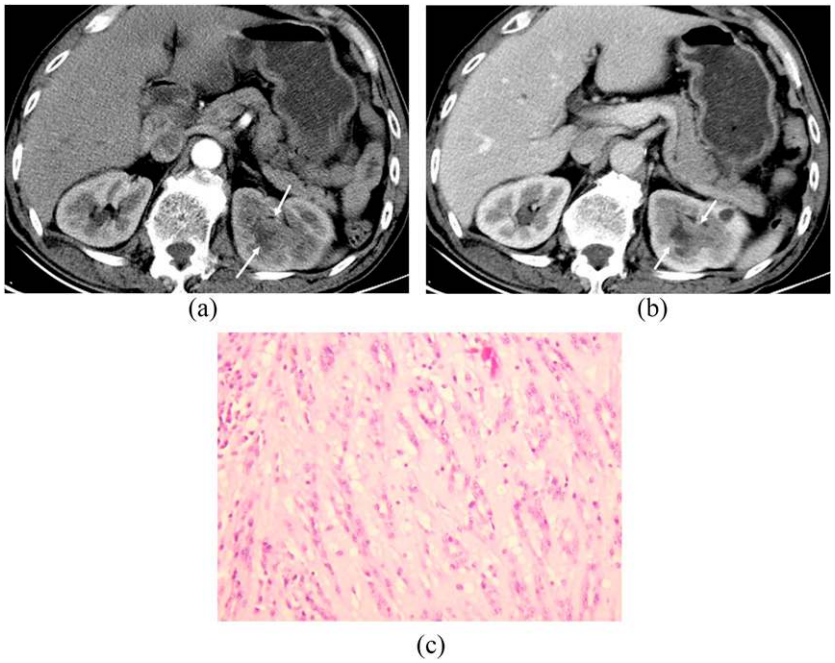

Figure 3. (a–d) Collecting duct carcinoma of the right kidney in a 30-year-old female. Axial unenhanced CT image (a) shows an isodense mass in the medulla (black arrow); attenuation of the mass was 46 HU, and a cystic component was noted (white arrow). Axial image (b) shows moderate, heterogeneous enhancement (62 HU, black and white arrows) in the corticomedullary phase. In the nephrographic phase (c), attenuation of the tumour increased to 92 HU (black and white arrows). Haematoxylin and eosin stain (d) shows tumour cells exhibiting a tubular and papillary growth pattern (original magnification, ×400).

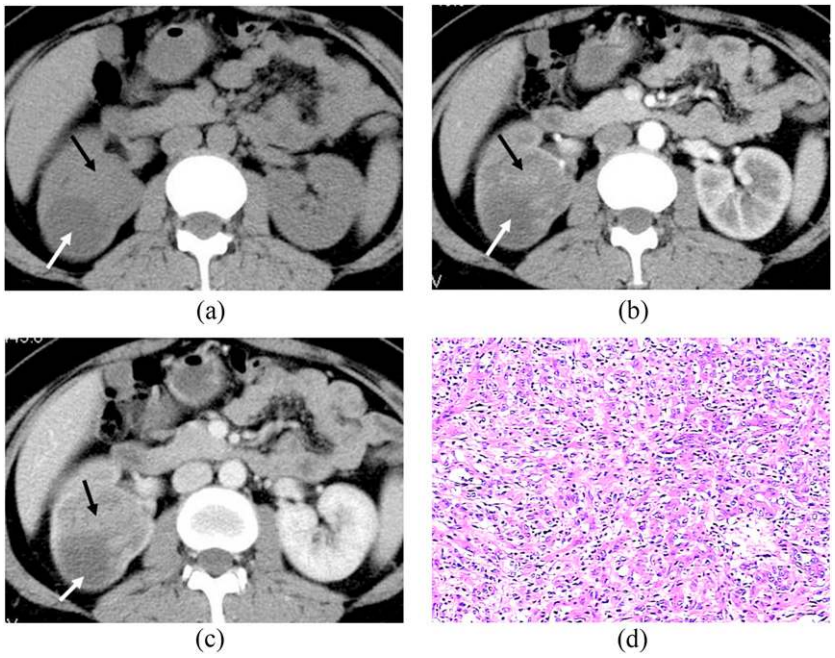

tubular, papillary, tubulopapillary, pseudopapillary, cribriform and solid patterns.[7] The tumour cells strongly express vimentin, 34βE12, CK19, CK8/18 etc., similar to MTSCC.

It is interesting that MTSCC and CDC share similar oncogenic and histological features and some imaging findings such as their medullary location, hypovascular enhancement pattern,

Figure 4. (a–d) Collecting duct carcinoma of the left kidney in a 46-year-old male. Axial unenhanced CT image (a) shows a clearly defined hyperdense mass (52 HU, arrow) in the renal medulla. Axial contrast-enhanced CT image (b) shows mild enhancement (71 HU) in the corticomedullary phase, which is less than the enhancement of the cortex and the medulla; tumour has a clear boundary (arrow). Axial image (c) shows increased attenuation of the tumour (93 HU) in the nephrographic phase (arrow). Haematoxylin and eosin stain (d) shows tumour cells exhibiting a tubular and tubulopapillary growth pattern (original magnification, ×400).

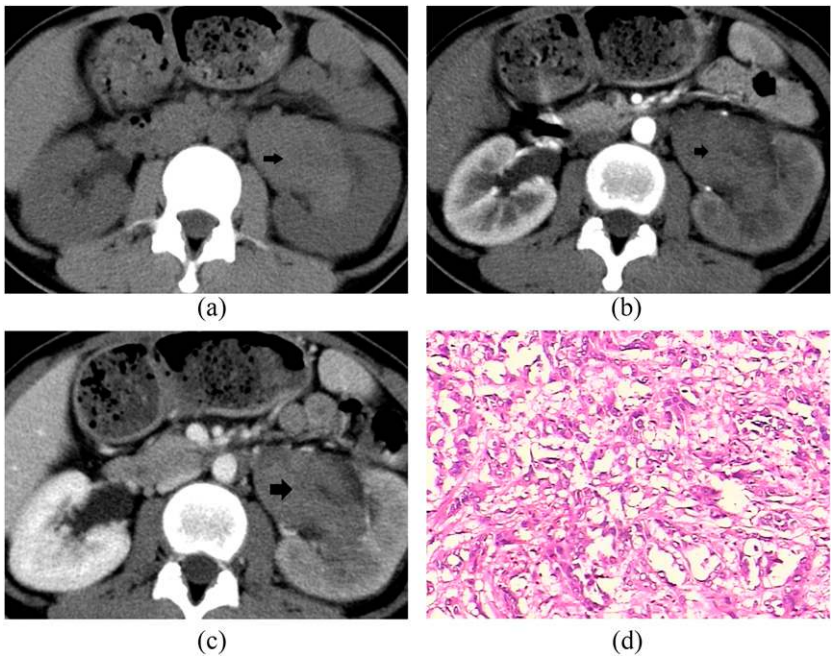

infiltrative pattern of growth etc. Although MTSCC and CDC have been relatively well described in pathological studies,[7–9] comparative studies of CT appearances are scant, particularly in combination with histopathological examination. In routine clinical work, the rate of correct differential diagnosis on imaging is low for MTSCC[9] and CDC. This is likely due to both a low incidence and a low level of awareness. Thus, there is a relative dearth of comparative imaging characterization of these two tumours. Moreover, patients with MTSCC have a better prognosis than CDC after total nephrectomy or local resection.[10] The prognosis of MTSCC seems to be favourable; only one example has been reported with metastasis, and this tumour is best considered as a low-grade carcinoma.[10] CDCs are now widely regarded as a more aggressive variant carcinoma. The prognosis is poor with many being metastatic at presentation. Thus, an accurate diagnosing is important for guiding the clinical treatment. Our data suggest a constellation of imaging features that can help identify the two tumour subsets. CDC is visualized as a hyperdense mass, whereas MTSCC is seen as an isodense or hypodense mass on unenhanced CT. The enhancement degree of MTSCC is lower than CDC during all phases.

Histopathologically, MTSCC and CDC arise from the medulla, which distinguish them from the typical clear cell RCCs that arise from the renal cortex. Imaging and surgery show that small MTSCC and CDC are located in the medulla, whereas a large tumour can displace the renal pelvis, grow into the renal cortex and even protrude through the renal capsule.[11] Both lymph node and distant metastases can occur.[12] Other types of tumours may also involve the renal medulla, *e.g.* parts of clear cell RCC,[13,14] transitional cell carcinoma,[15] squamous cell carcinoma[16] and chromophobe RCC.[17] It is difficult to differentiate MTSCCs and CDCs from other tumours if only relying on tumour position. Other characteristics may be helpful, *e.g.* about 94% of cortical clear cell RCCs, the most common subtype, exhibit an expansible appearance with exophytic growth that disrupts the reniform contour,[18] and enhancement is often similar to the cortex. Transitional cell carcinomas arise from the collecting system and may cause hydronephrosis.[19] Chromophobe RCCs may have a spoke-like pattern in some cases. Segmental enhancement inversion was found to be a characteristic enhancement pattern of renal oncocytoma.

Attenuation of renal parenchyma typically ranges from 30 to 40 HU on unenhanced CT scan; a hyperattenuating renal mass is higher than that of the surrounding renal parenchyma and is at least 40 HU but commonly no higher than 90 HU.[20,21] Our results show that CDCs appear as hyperattenuating solid tumours, whereas MTSCCs appear as isodense or hypodense masses. Other authors[22,23] reported that the pathological basis for hyperdense appearance of a tumour on unenhanced CT was mainly minimal intratumoral haemorrhage (haemosiderin deposition). On pathology, we found nine cases (50%) of CDC, whereas only one case (5%) of MTSCC with intratumoral haemorrhage (haemosiderin deposition) ($p = 0.002$). This pattern is different from tumours with high-attenuation solid masses including clear cell RCCs, angiomyolipomas with minimal fat,[24] oncocytomas[25] and papillary RCCs. RCCs >3 cm often contain intratumoral necrosis, haemorrhage, cystic components and calcifications and are usually of the clear cell variety.[26] Papillary RCCs are commonly homogeneous, when poorly differentiated, but often have necrosis and cystic change and, in such a situation, may appear heterogeneous which is similar to CDC. However, papillary RCCs may be multifocal and bilateral and tend to be <2 cm in size at diagnosis and hypovascular.

In our study, MTSCC and CDC tumour enhancement was lower than the enhancement of normal renal cortex and medulla in all enhanced phases ($p < 0.001$). Enhancement was higher in CDC tumours than in MTSCC in all phases ($p = 0.011$, $p = 0.006$ and $p = 0.052$, respectively). This enhancement pattern is atypical of tumours with hypervascularity such as clear cell RCCs,[27] renal medullary carcinomas,[28] renal angiomyolipomas and renal angiomas.[29]

Renal medullary carcinoma is seen in young people (mean age 22 years) with sickle-cell trait. It is often possible to anticipate the correct diagnosis with imaging studies. Metastatic deposits such as cervical nodes or brain tumour may be the initial evidence of disease. Centrally located tumours with an infiltrative growth pattern, invading renal sinus, are typical. Caliectasis without pelviectasis and tumour encasing the pelvis are also described.[28] The degree of enhancement of clear cell RCCs is commonly higher than that of the renal cortex. These findings suggest that it may be relatively easy to distinguish MTSCC and CDC tumours with hypervascularity on the basis of differences in enhancement.

In common with MTSCC and CDC, papillary RCC, chromophobe RCCs and metanephric adenomas are hypovascular compared with the renal parenchyma on enhanced CT imaging.[30] The majority of papillary RCCs show mild enhancement during all enhanced phases. Furthermore, papillary RCCs may be multifocal and bilateral and tend to be <2 cm in size at diagnosis; less enhancement and a direct comparison study would be helpful dissimilar to that seen with MTSCC and CDC. Chromophobe RCCs may have a spoke-like pattern in some cases.

Most renal tumours in general grow by radial expansion with displacement of the normal parenchyma, focal bulging of the renal contour and pseudocapsule formation. Infiltrative growth was a less common pattern, which differs from those of cortical clear cell RCCs, the most common subtype, which exhibit an expansible appearance with exophytic growth that disrupts the reniform contour.[31] In our study, only three cases with MTSCC (14%) and four cases with CDC (22%) had obvious complete or near-complete boundaries on CT scan (capsule sign), which was best seen in the delayed phase. This is consistent with previous pathological and surgical findings,[31] and it may be a feature that distinguishes MTSCC and CDC from papillary RCC, well-differentiated clear cell RCC, chromophobe RCC, Wilm's tumour and RCC associated with Xp11.2 translocation/*TFE* gene fusion, all of which have a clear boundary.

Retroperitoneal lymph node metastasis was noted in no cases with MTSCC and five cases with CDC (28%, $p = 0.015$). MTSCC and CDC rarely invade into the renal pelvis, calyx or renal vein, whereas clear cell RCC more commonly invades into

inferior vena cava or ureter. Clear cell RCC is commonly associated with lymph node metastasis and renal vein infiltration. Hence, different biological behaviours of the tumours may also provide useful diagnostic information.

RCC, the most common neoplasm of the adult kidney accounts for 2–3% of all malignant diseases in adults. Although imaging techniques for abdominal screening have increased the incidental detection of renal tumours, 25–30% of patients still have metastases at presentation. Metastatic RCC is one of the most treatment-resistant malignancies, and patients have a dismal prognosis with a <10% 5-year survival rate. The identification of markers that can predict potential metastases will have a great impact on improving the patient's outcome. A novel monoclonal antibody raised against bilitranslocase has been proposed for use as a marker of transition from normal tissue to neoplastic transformation in human kidney.[32]

Information regarding the clinical behaviour of these two tumours is limited owing to their rare incidence. All of our 21 patients with MTSCC were alive without manifesting disease or any other signs or symptoms during 5–13 years of follow-up. However, out of 18 patients with CDC, 7 patients (39%) expired within 5 years of the initial diagnosis, whereas the others are currently still alive. Although the clinical course of these patients is rather indolent, routine follow-up is still mandatory. The correct distinction of these tumours can lead to better understanding of their clinicopathological differences, which should aid in developing individualized management plans.

Our study has several limitations. First, pathological specimens were sectioned in a variety of planes, but only axial, sagittal and coronal planes were available on CT images. Therefore, it was difficult to meticulously correlate the imaging findings with the histopathological figures. Second, few patients were included in the study, and finally, the retrospective nature of this study might have introduced some form of patient selection bias.

In conclusion, MTSCC and CDC are both rare subtypes of RCC with special pathological features. Precise diagnosis based on CT imaging findings alone remains difficult. However, we clearly demonstrated imaging features that may help to distinguish the two tumour types. Further research is needed to verify our findings in larger patient populations.

FUNDING

The authors received funding from National Natural Science Foundation of China: 81401384.

REFERENCES

1. Parwani AV, Husain AN, Epstein JI, Beckwith JB, Argani P. Low grade myxoid renal epithelial neoplasms with distal nephron differentiation. *Hum Pathol* 2001; **32**: 506–12. doi: 10.1053/hupa.2001.24320
2. Fine SW, Argani P, DeMarzo AM, Delahunt B, Sebo TJ, Reuter VE, et al. Expanding the histologic spectrum of mucinous tubular and spindle cell carcinoma of the kidney. *Am J Surg Pathol* 2006; **30**: 1554–60. doi: 10.1097/01.pas.0000213271.15221.e3
3. Lopez-Beltran A, Scarpelli M, Montironi R, Kirkali Z. 2004 WHO classification of the renal tumors of the adults. *Eur Urol* 2006; **49**: 798–805. doi: 10.1016/j.eururo.2005.11.035
4. Paner GP, Srigley JR, Radhakrishnan A, Cohen C, Skinnider BF, Tickoo SK, et al. Immunohistochemical analysis of mucinous tubular and spindle cell carcinoma and papillary renal cell carcinoma of the kidney: significant immunophenotypic overlap warrants diagnostic caution. *Am J Surg Pathol* 2006; **30**: 13–19. doi: 10.1097/01.pas.0000180443.94645.50
5. Eren S, Karaman A, Okur A. The superior vena cava syndrome caused by malignant disease. Imaging with multi-detector row CT. *Eur J Radiol* 2006; **59**: 93–103. doi: 10.1016/j.ejrad.2006.01.003
6. Nanpo Y, Fujii R, Nishizawa S, Sasaki Y, Kodama Y, Matsumura N, et al. A case of collecting duct carcinoma originating from renal cyst. [In Japanese.] *Hinyokika Kiyo* 2013; **59**: 11–15.
7. Amin MB, Smith SC, Agaimy A, Argani P, Compérat EM, Delahunt B, et al. Collecting duct carcinoma *versus* renal medullary carcinoma: an appeal for nosologic and biological clarity. *Am J Surg Pathol* 2014; **38**: 871–4. doi: 10.1097/PAS.0000000000000222
8. Grigore A, Toma L, Stoicea M, Dinu M, Ardeleanu C. Rare renal tumor—mucinous tubular and spindle cell carcinoma. *Rom J Morphol Embryol* 2012; **53**: 167–71.
9. Song HJ, Ma J, Zhou HB, Ma HH, Shi QL, Zhou XJ. Mucinous tubular and spindle cell carcinoma of kidney: a clinicopathological study. [In Chinese.] *Zhonghua Bing Li Xue Za Zhi* 2011; **40**: 444–8.
10. Sarsik B, Sımşır A, Karaarslan S, Sen S. Mucinous tubular and spindle cell carcinoma of kidney and problems in diagnosis. *Turk Patoloji Derg* 2011; **27**: 116–26. doi: 10.5146/tjpath.2011.01059
11. Makni SK, Chaari C, Ellouze S, Ayadi L, Charfi S, Abbes K, et al. Mucinous tubular and spindle cell carcinoma of the kidney associated with tuberculosis. *Saudi J Kidney Dis Transpl* 2011; **22**: 335–8.
12. Algaba F, Akaza H, López-Beltrán A, Martignoni G, Moch H, Montironi R, et al. Current pathology keys of renal cell carcinoma. *Eur Urol* 2011; **60**: 634–43. doi: 10.1016/j.eururo.2011.06.047
13. Sauk SC, Hsu MS, Margolis DJ, Lu DS, Rao NP, Belldegrun AS, et al. Clear cell renal cell carcinoma: multiphasic multidetector CT imaging features help predict genetic karyotypes. *Radiology* 2011; **261**: 854–62. doi: 10.1148/radiol.11101508
14. Ruppert-Kohlmayr AJ, Uggowitzer M, Meissnitzer T, Ruppert G. Differentiation of renal clear cell carcinoma and renal papillary carcinoma using quantitative CT enhancement parameters. *AJR Am J Roentgenol* 2004; **183**: 1387–91. doi: 10.2214/ajr.183.5.1831387
15. Barrascout E, Beuselinck B, Ayllon J, Bättig B, Moch H, Teghom C, et al. Complete remission of pulmonary metastases of Bellini duct carcinoma with cisplatin, gemcitabine and bevacizumab. *Am J Case Rep* 2012; **13**: 1–2. doi: 10.12659/AJCR.882234
16. Yoon SK, Nam KJ, Rha SH, Kim JK, Cho KS, Kim B, et al. Collecting duct carcinoma of the kidney: CT and pathologic correlation. *Eur J Radiol* 2006; **57**: 453–60. doi: 10.1016/j.ejrad.2005.09.009
17. Rumpelt HJ, Störkel S, Moll R, Schärfe T, Thoenes W. Bellini duct carcinoma: further

evidence of this rare variant of renal cell carcinoma. *Histopathology* 1991; **18**: 115–22. doi: 10.1111/j.1365-2559.1991.tb01453.x

18. Pickhardt PJ, Siegel CL, Mclarney JK. Collecting duct carcinoma of the kidney: are imaging findings suggestive of the diagnosis? *AJR Am J Roentgenol* 2001; **176**: 627–33. doi: 10.2214/ajr.176.3.1760627
19. McDaid J, Farkash EA, Steele DJ, Martins PN, Kotton CN, Elias N, et al. Transitional cell carcinoma arising within a pediatric donor renal transplant in association with BK nephropathy. *Transplantation* 2013; **95**: e28–30. doi: 10.1097/TP.0b013e31828235ec
20. Silverman SG, Mortele KJ, Tuncali K, Jinzaki M, Cibas ES. Hyperattenuating renal masses: etiologies, pathogenesis, and imaging evaluation. *Radiographics* 2007; **27**: 1131–43. doi: 10.1148/rg.274065147
21. Zhu QQ, Wang ZQ, Zhu WR, Chen WX, Wu JT. The multislice CT findings of renal carcinoma associated with XP11.2 translocation/TFE gene fusion and collecting duct carcinoma. *Acta Radiol* 2013; **54**: 355–62. doi: 10.1258/ar.2012.120255
22. Bose D, Das RN, Chatterjee U, Banerjee U. Collecting duct carcinoma: a rare malignancy. *J Cancer Res Ther* 2013; **9**: 94–5. doi: 10.4103/0973-1482.110387
23. Zhu Q, Wu J, Wang Z, Zhu W, Chen W, Wang S. The MSCT and MRI findings of collecting duct carcinoma. *Clin Radiol* 2013; **68**: 1002–7. doi: 10.1016/j.crad.2013.04.004
24. Low G, Sahi K, Dhliwayo H. Low T2 signal intensity on magnetic resonance imaging: a feature of minimal fat angiomyolipomas. *Int J Urol* 2012; **19**: 90–1. doi: 10.1111/j.1442-2042.2011.02885.x
25. Gakis G, Kramer U, Schilling D, Kruck S, Stenzl A, Schlemmer HP. Small renal oncocytomas: differentiation with multiphase CT. *Eur J Radiol* 2011; **80**: 274–8. doi: 10.1016/j.ejrad.2010.06.049
26. Goyal R, Gersbach E, Yang XJ, Rohan SM. Differential diagnosis of renal tumors with clear cytoplasm: clinical relevance of renal tumor subclassification in the era of targeted therapies and personalized medicine. *Arch Pathol Lab Med* 2013; **137**: 467–80. doi: 10.5858/arpa.2012-0085-RA
27. Bata P, Gyebnar J, Tarnoki DL, Tarnoki AD, Kekesi D, Szendroi A, et al. Clear cell renal cell carcinoma and papillary renal cell carcinoma: differentiation of distinct histological types with multiphase CT. *Diagn Interv Radiol* 2013; **19**: 387–92. doi: 10.5152/dir.2013.13068
28. Blitman NM, Berkenblit RG, Rozenblit AM, Levin TL. Renal medullary carcinoma: CT and MRI features. *AJR Am J Roentgenol* 2005; **185**: 268–72. doi: 10.2214/ajr.185.1.01850268
29. Abercrombie JF, Holmes SA, Ball AJ. Diagnosis and management of renal angioma. *J R Soc Med* 1992; **85**: 625–7.
30. Zhu Q, Zhu W, Wu J, Chen W, Wang S. The clinical and CT imaging features of metanephric adenoma. *Acta Radiol* 2014; **55**: 231–8. doi: 10.1177/0284185113493411
31. Gurel S, Narra V, Elsayes KM, Siegel CL, Chen ZE, Brown JJ. Subtypes of renal cell carcinoma: MRI and pathological features. *Diagn Interv Radiol* 2013; **19**: 304–11. doi: 10.5152/dir.2013.147
32. Montanic S, Terdoslavich M, Rajcevic U, De Leo L, Bonin S, Serbec VC, et al. Development and characterization of a novel mAb against bilitranslocase—a new biomarker of renal carcinoma. *Radiol Oncol* 2013; **47**: 128–37. doi: 10.2478/raon-2013-0026